Traffic 2005; **6:** 1002–1013
Blackwell Munksgaard

doi: 10.1111/j.1600-0854.2005.00331.x

A Protein Kinase CK2 Site Flanking the Nuclear Targeting Signal Enhances Nuclear Transport of Human Cytomegalovirus ppUL44

Gualtiero Alvisi[1,2], David A. Jans[2,3], Jinjin Guo[4], Lorenzo A. Pinna[5] and Alessandro Ripalti[1,6,*]

[1]Dipartimento di Medicina Clinica Specialistica e Sperimentale, Sezione di Microbiologia, Università degli Studi di Bologna, Bologna, Italy
[2]Nuclear Signalling Laboratory, Department of Biochemistry and Molecular Biology, Monash University, Clayton, VIC 3168, Australia
[3]ARC Centre of Excellence for Biotechnology and Development
[4]Virus Laboratory, Second Clinical College, China Medical University, Shenyang, Liaoning, China
[5]Dipartimento di Chimica Biologica, Università di Padova, Padova, Italy
[6]Azienda Ospedaliera Universitaria di Bologna Policlinico S. Orsola–Malpighi, Dipartimento di Patologia Clinica, Microbiologia, e Medicina Trasfusionale – Unità Operativa di Microbiologia, Bologna, Italy
** Corresponding author: Alessandro Ripalti, aripa@med.unibo.it*

Received 27 April 2005, revised and accepted for publication 8 July 2005, published on-line 8 August 2005

The processivity factor of the human cytomegalovirus (HCMV) DNA polymerase phosphoprotein ppUL44 plays an essential role in viral replication, showing nuclear localization in infected cells. The present study examines ppUL44's nuclear import pathway for the first time, ectopic expression of ppUL44 revealing a strong nuclear localization in transfected COS-7 and other cell types, implying that no other HCMV proteins are required for nuclear transportation and retention. We show that of the two potential nuclear localization signals (NLSs) located at amino acids 162–168 (NLS1) and 425–431 (NLS2), NLS2 is necessary and sufficient to confer nuclear localization. Moreover, using enzyme-linked immunosorbent assays and gel mobility shift assays, we show that NLS2 is recognized with high affinity by the importin (IMP) α/β heterodimer. Using gel mobility shift and transient transfection assays, we find that flanking sequences containing a cluster of potential phosphorylation sites, including a consensus site for protein kinase CK2 (CK2) at Ser[413] upstream of the NLS, increase NLS2-dependent IMP binding and nuclear localization, suggesting a role for these sites in enhancing UL44 nuclear transport. Results from site-directed mutagenic analysis and live-cell imaging of green fluorescent protein (GFP)-UL44 fusion protein-expressing cells treated with the CK2-specific inhibitor 4,5,6,7-tetrabromobenzotriazole are consistent with phosphorylation of Ser[413] enhancing ppUL44 nuclear transport.

Key words: CK2, DNA polymerase, GFP, HCMV, NLS, nuclear transport, phosphorylation, SV-40, T-ag, UL44

The β-*herpesviridae* subfamily member human cytomegalovirus (HCMV) is a major human pathogen (1). Replication of its double-stranded DNA (dsDNA) genome occurs in the nuclei of infected cells via a rolling circle process mediated by 11 virally-encoded proteins (2,3). The product of ORF UL44 (ppUL44) is readily detectable by Western blot as a family of proteins in lysates of infected cells – its most abundant member is a 52-kDa phosphoprotein of 433 amino acids – with a strong dsDNA-binding ability (4,5). The protein is phosphorylated by pUL97, a viral-encoded kinase (6,7) and by at least one host cell kinase (7). During viral infection, ppUL44 localizes in the nucleus of infected cells (8), where it is thought to interact with the product of ORF UL54, the catalytic subunit of the viral DNA polymerase, to confer processivity to the DNA polymerase holoenzyme (9).

Defined as a 'polymerase accessory protein' (PAP), an essential factor for DNA replication (10,11), ppUL44 and its homologues are highly conserved among herpesviruses (12). The catalytic activity of ppUL44 resides in the N-terminal portion as deletion of amino acids 291–433 does not alter its known biochemical properties (5,13). The role of the C-terminus of ppUL44 in HCMV infection remains to be elucidated (14). Significantly, the last 24 amino acids of several β-herpesvirus PAPs, including those from HCMV, murine CMV, human herpesvirus 6 (HHV-6) and HHV-7, are extremely well conserved, all harbouring putative or confirmed nuclear localization signals (NLSs) preceded by potential protein kinase CK2 (CK2) phosphorylation sites (15,16).

Molecules of >45 kDa cannot diffuse passively into the nucleus through the aqueous channel delimited by the nuclear pore complex (NPC), instead being actively translocated into the nucleus in NLS-dependent fashion through the action of members of the importin (IMP) superfamily of intracellular transporters (17). The IMPs mediate docking of the NLS-containing protein to the NPC and its translocation through it into the nucleus. Most NLSs consist of a single cluster of basic amino acids such as that of the simian virus SV40 large tumour antigen (T-ag) (18), which is recognized by the IMPα/β heterodimer, where IMPα recognizes the NLS, and IMPβ facilitates the IMPα–NLS interaction by effecting a

conformational change in IMPα to release an autoinhibitory domain from the IMPα NLS-binding site, thereby greatly increasing the affinity of the interaction (19). IMP β subsequently mediates interaction with NPC components to facilitate passage through the NPC, and then with the guanine nucleotide-binding protein Ran, to achieve cargo release in the nucleus (17). NLS-dependent nuclear import is often regulated by phosphorylation through a number of specific mechanisms (17,20). In the case of T-ag, the modular CcN motif confers phosphorylation signal transduction-responsive NLS-dependent nuclear localization through CK2 and cyclin-dependent kinase (cdk) phosphorylation sites (21–24).

Although functional NLSs have been described within ppUL44 homologues (15,16,25), sequences responsible for the nuclear transport of ppUL44 have not yet been described. The aim of the present study is to identify candidate NLSs within ppUL44, to define their role in ppUL44 nuclear import pathway and to ascertain whether their activity may be influenced by phosphorylation. Our results define the C2N motif, reminiscent of the CcN motif of T-ag, responsible for CK2-enhanced and IMPα/β-dependent nuclear import of ppUL44.

Results

ppUL44 nuclear localization is dependent on NLS2

Examination of the primary sequence of ppUL44 indicated the presence of the putative basic NLSs PHTRVKR[168] (NLS1) and PNTKKQK[431] (NLS2) (Figure 1). To test whether NLS1 or NLS2 may play a role in ppUL44 nuclear transport, we transfected COS-7 cells with UL44-encoding constructs. Immunostaining indicated nuclear localization of ppUL44 and ppUL44ΔNLS1, but cytoplasmic localization of ppUL44ΔNLS2 (Figure 1). Similar results were obtained after transfection of U373-MG cells (data not shown). Results were confirmed by performing live-cell imaging using confocal laser scanning microscopy (CLSM; BioRAD MRC500, Hercules, CA) on COS-7 cells transfected to express green fluorescent protein (GFP)-UL44 fusion proteins with the GFP-β-galactosidase (Gal) and GFP-T-ag-NLS-β-Gal-encoding constructs pHM830 and pHM830-T-ag as negative and positive controls, respectively. GFP-T-ag-NLS-β-Gal, GFP-UL44 and UL44ΔNLS1 all showed nuclear localization in transfected cells, whereas UL44ΔNLS2 showed cytosolic fluorescence comparable with that seen for GFP-β-Gal alone (Figure 2A,B). The clear implication was that NLS2 but not NLS1 was necessary for ppUL44 nuclear localization.

ppUL44-NLS2 is sufficient to target GFP to the nucleus

To determine whether the ppUL44-NLS2, out of the context of the ppUL44 molecule, was capable of directing the heterologous GFP protein to the nucleus, COS-7 cells were transfected to express GFP-UL44NLS1, GFP-UL44NLS2, GFP-UL44NLS1Δ and GFP-UL44NLS2Δ fusion proteins and imaged live using CLSM 16 h post-transfection (Figure 3A). As a control, cells were transfected to express GFP alone, a 27-kDa protein able to freely diffuse through the NPC, and thus distribute equally in nuclear and cytoplasmic compartments (26). Confocal images were analysed quantitatively for the nuclear to cytoplasmic ratio (Fn/c). No marked difference between cells transfected to express GFP, GFP-UL44NLS1, GFP-UL44NLS1Δ and GFP-UL44NLS2Δ was observed, but cells expressing GFP-UL44NLS2 showed significantly higher nuclear accumulation, with an Fn/c of 3.2 significantly higher ($p < 0.0001$) than that observed for GFP alone (Fn/c of 1.9) (Figure 3B). Thus, ppUL44-NLS2 but not ppUL44-NLS1 was sufficient to confer nuclear accumulation on GFP. That GFP-UL44NLS2Δ protein showed a significant reduction in nuclear accumulation (Fn/c of 2) compared with GFP-UL44NLS2 implied that the basic

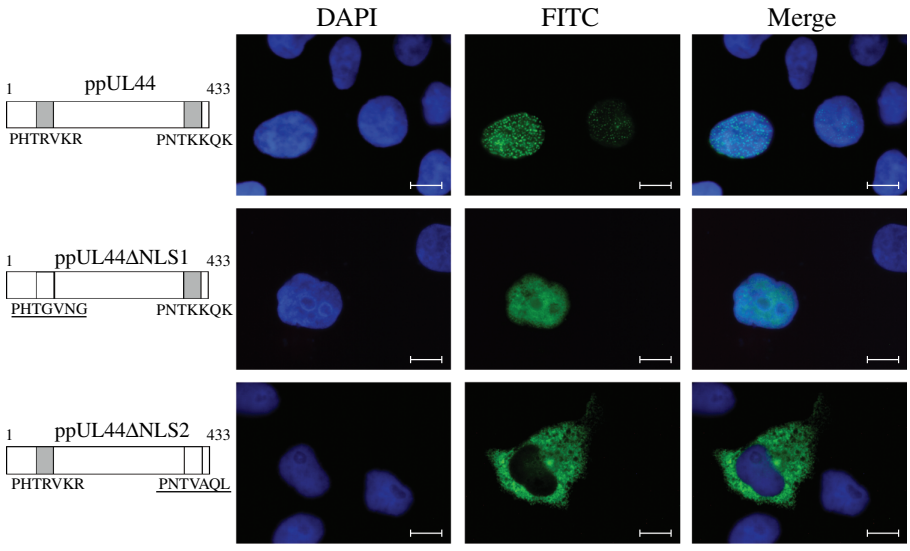

Figure 1: Subcellular localization of ppUL44 wild-type protein and NLS1 and NLS2 mutants. COS-7 cells transfected with constructs encoding ppUL44 carrying site-specific mutations were processed for immunofluorescence 16 h post-transfection as described in *Materials and Methods*. Scale bars represent 25 μm. NLS, nuclear localization signal.

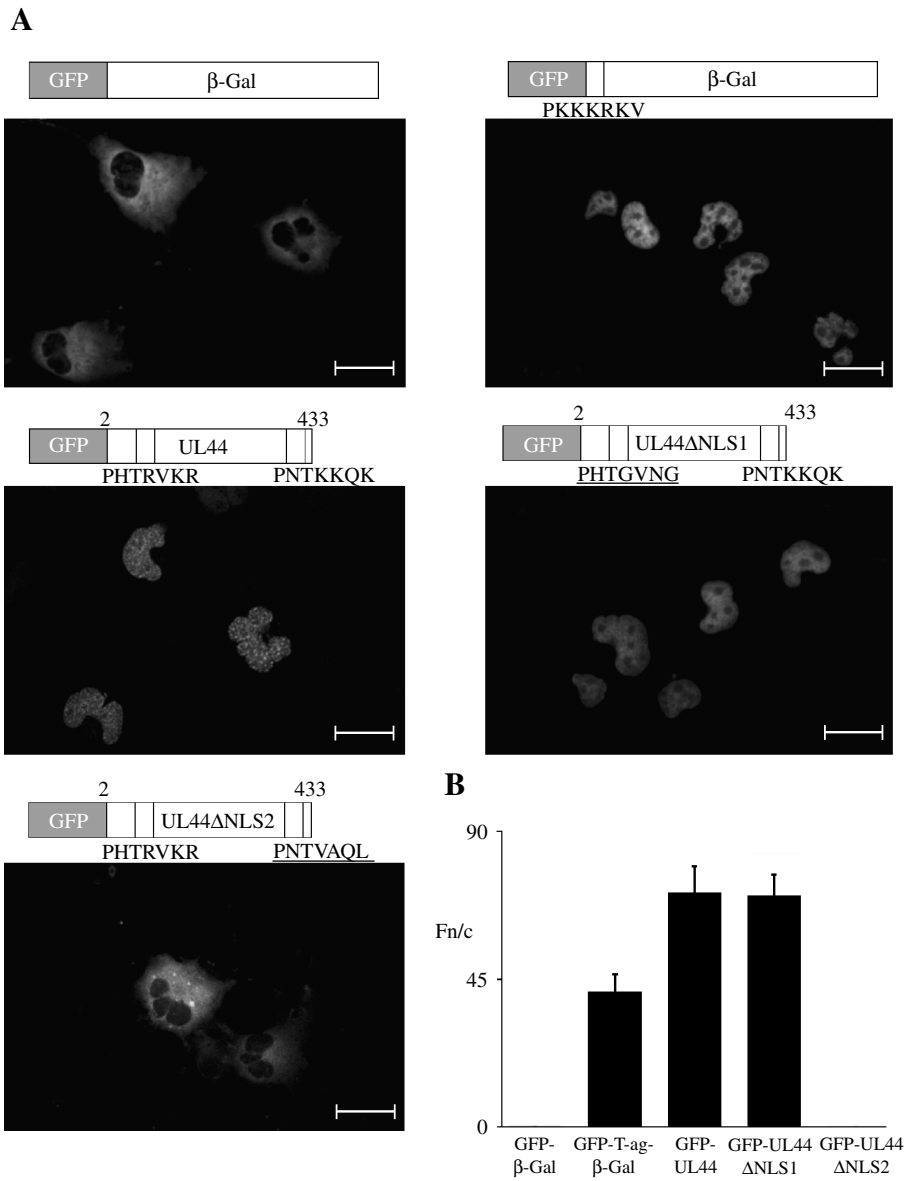

Figure 2: ppUL44-NLS2 but not ppUL44-NLS1 is necessary for nuclear accumulation of ppUL44. (A) COS-7 cells were transfected to express GFP fusion proteins and imaged live 16 h after transfection using confocal laser scanning microscopy (CLSM) and a 40× water immersion objective. (B) Quantitative results for the nuclear to cytoplasmic ratio (Fn/c) for GFP-UL44 fusion proteins. Confocal images such as those shown in Figure 2A were analysed as described in *Materials and Methods* using the IMAGE J software. Data represent the mean ± SEM ($n > 40$). Scale bars represent 50 μm. GFP, green fluorescent protein; NLS, nuclear localization signal.

residues of NLS2 were critical for this nuclear targeting function. Similar results were obtained after transfection of HeLa cells (data not shown).

ppUL44 is recognized with high affinity by IMPα/β

To test whether NLS2 and/or NLS1 were able to bind IMPs, the His_6GFP-UL44NLS1 and His_6GFP-UL44NLS2 fusion proteins were subjected to native gel electrophoresis without and with preincubation with different IMP combinations (Figure 4). In the absence of IMPs, His_6GFP-UL44NLS1 and His_6GFP-UL44NLS2 fusion proteins migrated with similar mobility on the native gel. Results for preincubation with IMPs showed that His_6GFP-UL44NLS2 was able to interact specifically with both IMPα and IMPα/β in contrast to His_6GFP-UL44NLS1, on the basis of altered mobility in the native gel (Figure 4). To confirm these observations, enzyme-linked immunosorbent assay (ELISA)-based binding assays were performed to test the ability of bacterially expressed His_6-tagged UL44 proteins to interact with IMPs (Figure 5). His_6UL44 and His_6UL44ΔNLS1 showed a very high affinity interaction with the IMPα/β heterodimer (left panel), exhibiting apparent dissociation constants (K_d) of approximately 2 nM. IMPα bound to the UL44 proteins with high affinity (K_d of approximately 20 nM, central panel), while IMPβ bound to the UL44 proteins

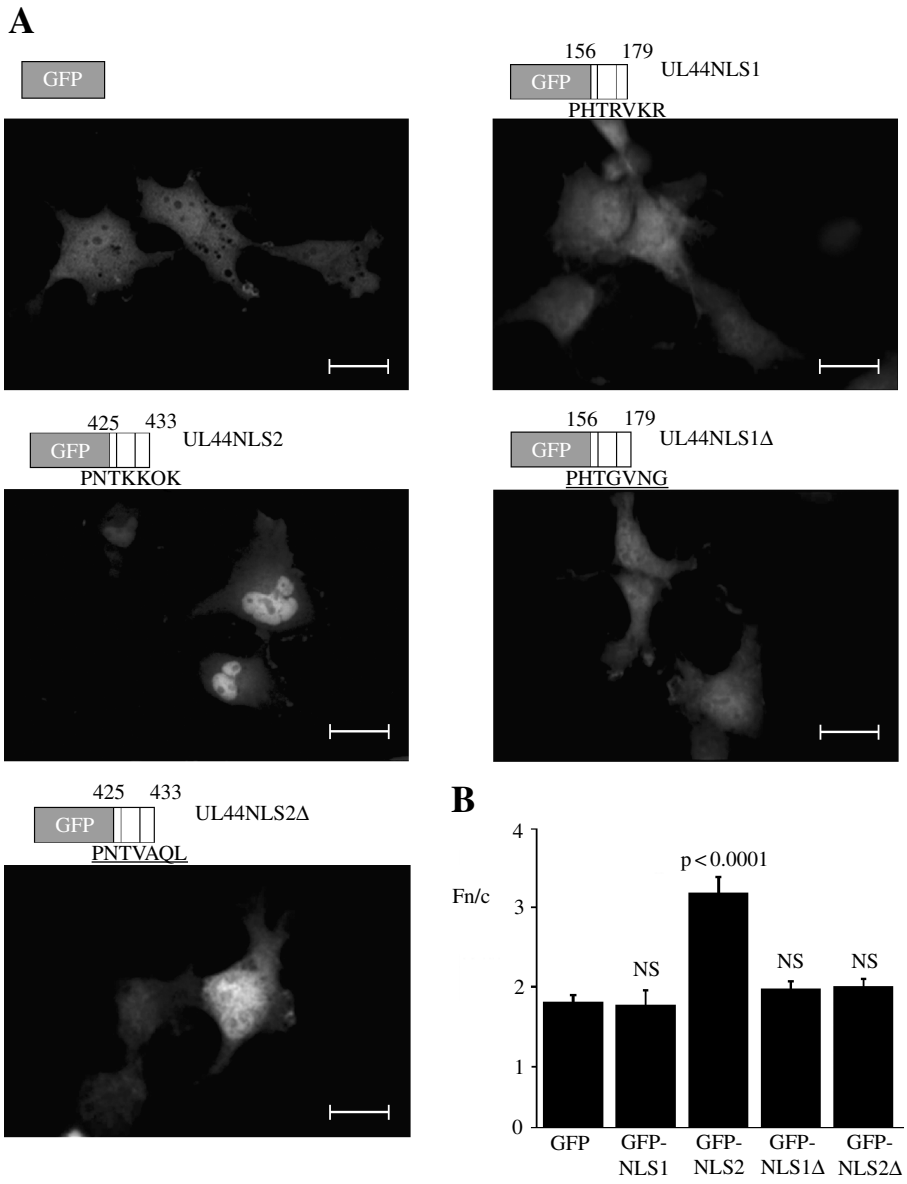

Figure 3: ppUL44-NLS2 but not ppUL44-NLS1 is sufficient to target green fluorescent protein (GFP) to the nucleus. (A) COS-7 cells were transfected to express GFP fusion proteins and imaged live 16 h after transfection using confocal laser scanning microscopy (CLSM) and a 40× water immersion objective. (B) Quantitative results for the nuclear to cytoplasmic ratio (Fn/c) for GFP-UL44NLS fusion proteins, performed as described in the legend to Figure 2. Data represent the mean ± SEM ($n > 40$) with p-values for the test of significance between the Fn/c-values for the proteins indicated compared to GFP. NS = not significant. Scale bars represent 50 μm. NLS, nuclear localization signal.

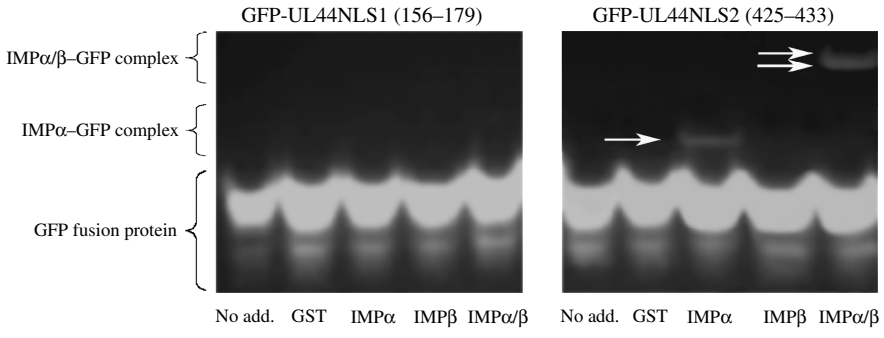

Figure 4: ppUL44-NLS2 confers specific importin (IMP) binding. The indicated GFP fusion proteins were incubated as described in *Materials and Methods* in the absence or presence of 10 μM of glutathione *S*-transferase (GST) and GST-IMPs prior to native gel electrophoresis. Arrows indicate the positions of GFP fusion proteins and fusion protein–IMP complexes. GFP, green fluorescent protein; NLS, nuclear localization signal.

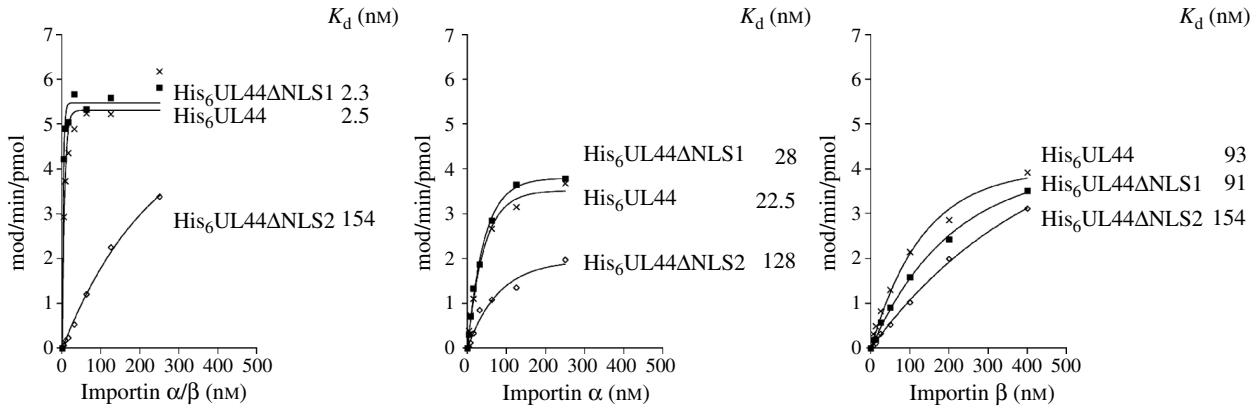

Figure 5: ppUL44-NLS2 is recognized with high affinity by the importin (IMP) α/β heterodimer. An ELISA-based binding assay was performed in which fusion proteins His_6UL44, His_6UL44ΔNLS1 and His_6UL44ΔNLS2 were coated onto microtitre plates and incubated with increasing concentrations of mouse IMPα/β (left panel), α (centre) or β (right) followed by successive incubation with primary and secondary antibodies and chromogenic substrate. Data were fitted to the function $B(x) = B_{max}(1 - e^{-kB})$, where x is the concentration of IMP, k is the rate constant and B is the level of IMP bound. The results are from a single typical experiment performed in triplicate. The values for the apparent K_d representing the IMP concentration yielding half-maximal binding are indicated. K_d, apparent dissociation constant; NLS, nuclear localization signal.

with only low affinity (K_d of approximately 100 nM, right panel). Mutation of basic residues within NLS2 resulted in remarkably reduced binding affinities between His_6UL44 and both IMPα and α/β (K_d of approximately 150 nM). The clear implication of the results for native polyacrylamide gel electrophoresis (PAGE) and the ELISA assays was that ppUL44 nuclear import was likely to be mediated by the IMPα/β heterodimer which specifically recognized NLS2 with very high affinity.

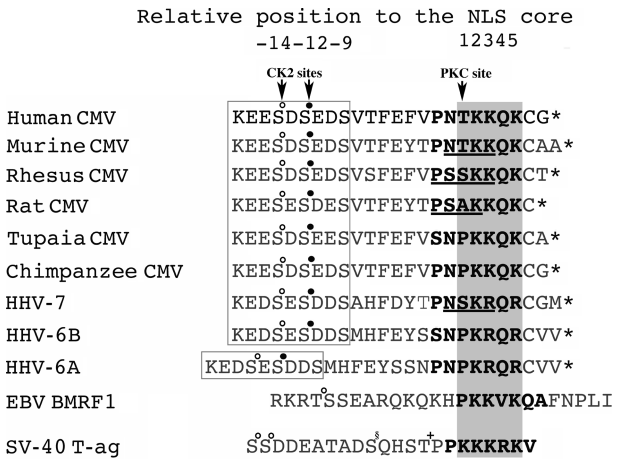

Figure 6: Human cytomegalovirus (HCMV) ppUL44 homologues share a well-conserved C-terminal motif, the C2N (CK2 and NLS) motif, which resembles the T-ag CcN motif. Putative nuclear localization signals (NLSs) are indicated in boldface type, with the NLS core indicated by grey boxes. White boxes indicate conserved CK2 consensus sequences. Putative PKC consensus sequences are underlined. (*) = C-terminus of the protein; (o) = CK2 putative phosphorylation site; (•) = CK2 putative phosphorylation site dependent on Ser^{418} phosphorylation; (§) = dsDNA-PK phosphorylation site; ($^+$) = p34 cdk phosphorylation site. Arrows indicate putative phosphorylation sites on ppUL44 sequence. The single-letter amino acid code is used. dsDNA-PK, double-stranded DNA-dependent protein kinase; PKC, protein kinase C; T-ag, tumour antigen.

Sequences upstream of UL44NLS2 modulate NLS2 activity

A putative CK2 phosphorylation site has been previously described upstream of putative NLS sequences on PAPs encoded by herpesviruses (15,16). Sequence alignments for HCMV ppUL44 and various viral homologues revealed a high degree of conservation over the 24 C-terminal amino acids, including NLS2 and several potential phosphorylation sites upstream and adjacent to the NLS (Figure 6). In particular, all homologues retain a Ser residue representing a potential phosphorylation site for CK2 activity at position −14 with respect to the NLS core. The consensus site for CK2 requires an acidic residue at the +3 position – acidic residues in +1/+2 and −1/−2/−3 positions increase the likelihood of phosphorylation – with phosphoserine/phosphothreonine able to substitute functionally for glutamic acid/aspartic acid in this respect (27). This means that phosphorylation at the serine at position −9, a putative target of phosphorylation according to the prediction software NETPHOS (Center for Biological Sequence Analysis, Technical University of Denmark, Lingby, Denmark) (score: 0.970) (28), would make the serine at position −12, a second potential site for CK2 phosphorylation. An exception with respect to the arrangement of CK2 sites upstream of the NLS is the HHV-6 A homologue, which possesses an additional two amino acids between the NLS and the phosphorylation sites, while Epstein–Barr virus BMRF1 is divergent, with only a single-consensus CK2 site in the form of the threonine at position −11. Five of eight ppUL44 homologues display one or two potential phosphorylation sites for protein kinase C at position +1 and/or −1 with respect to the NLS core.

Significantly, the 24 amino acid-conserved motif depicted in Figure 6 shows overall similarity to the T-ag CcN motif, where CK2 and a dsDNA-dependent protein kinase (dsDNA-PK) synergistically phosphorylates $Ser^{111/112}$ and Ser^{120} (22), respectively, to enhance NLS activity. By contrast, the cdk cdc2 phosphorylates Thr^{124}, adjacent to the NLS, to inhibit NLS-dependent nuclear import (24). We decided to name the motif present in ppUL44 and homologues the C2N (CK2 and NLS) motif, by analogy.

To test whether the sequences flanking the NLS within the ppUL44-C2N motif could regulate nuclear import, we compared the localization of GFP fused either to the C2N motif or to NLS2 alone in transfected live COS-7 cells (Figure 7A). Image analysis revealed significantly higher ($p < 0.0001$) levels of nuclear accumulation in the case of GFP-UL44C2N (Fn/c of 11.5), well over three times higher than that shown by GFP-UL44NLS2 (Figure 7B). Clearly, the sequences including the putative phosphorylation sites flanking NLS2 significantly enhance its activity.

To determine whether CK2 was involved in modulating the activity of ppUL44-NLS2 by phosphorylating Ser^{413}, we generated the C2N-Gly^{413} and C2N-Ala^{413} mutant derivatives and compared their localization in transfected live COS-7 cells (Figure 8A) in the absence (left panel) and presence of 4,5,6,7-tetrabromobenzotriazole (TBB), a selective inhibitor of CK2 (29) (right panel). GFP-T-ag-CcN, carrying the T-ag CcN motif, was used as a control. In the absence of TBB, both mutant derivatives showed a significantly impaired ($p < 0.003$) nuclear accumulation (Fn/c of approximately 7) when compared with the wild-type. In the presence of TBB, a significant reduction ($p = 0.0003$) of nuclear accumulation of GFP-C2N (Fn/c of 7.6), but not of C2N-Gly^{413} (Fn/c of 7.0) or C2N-Ala^{413} (Fn/c of 8.5), was observed. The Fn/c of the control protein GFP-T-ag-CcN was decreased approximately 40% ($p = 0.003$) by TBB treatment (Figure 8B). These results strongly suggest that CK2 enhances ppUL44 nuclear accumulation, with the results for the point mutant derivatives being consistent with Ser^{413} being the key phosphorylation site.

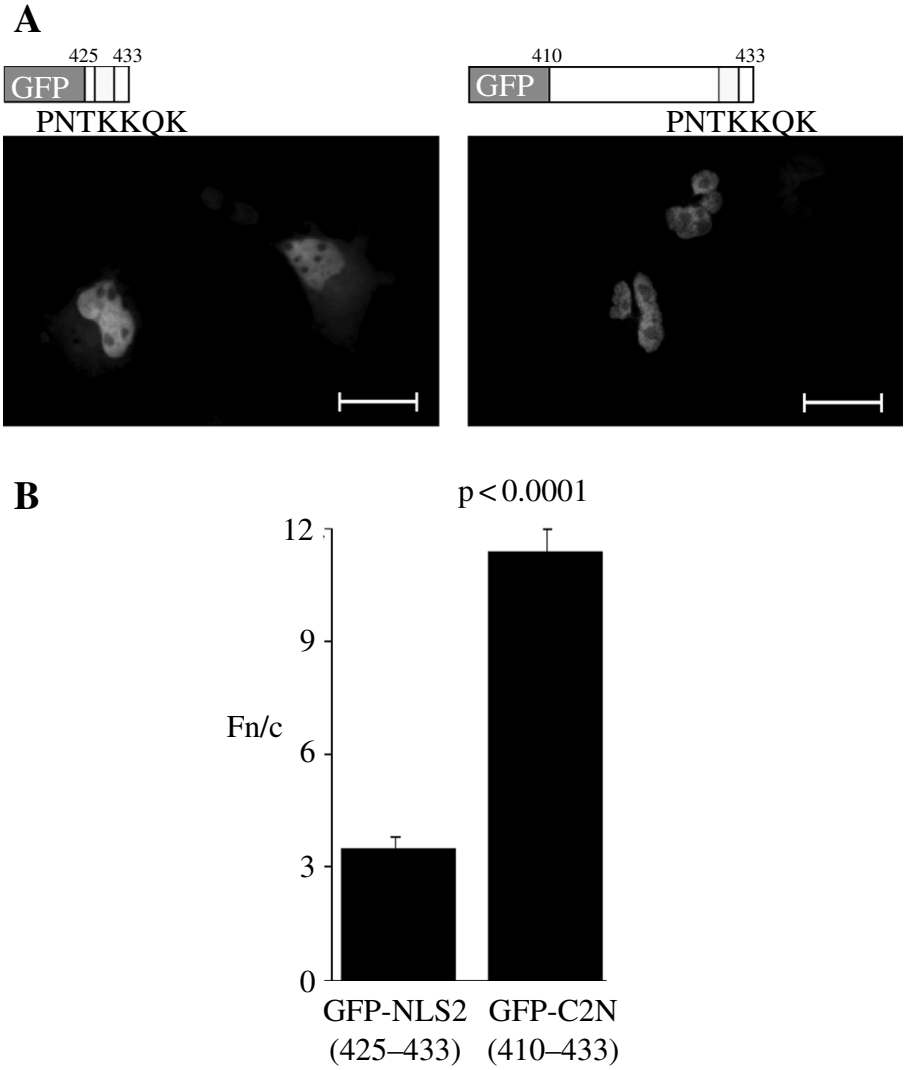

Figure 7: Upstream sequences enhance ppUL44-NLS2 activity. (A) COS-7 cells were transfected to express the indicated GFP fusion proteins and imaged live 16 h after transfection by using confocal laser scanning microscopy (CLSM) and a 40× water immersion objective. (B) Quantitative results for the nuclear to cytoplasmic ratio (Fn/c), performed as described in the legend to Figure 2. Data represent the mean ± SEM ($n > 40$), with p-values for the test of significance between the Fn/c-values for the proteins indicated. Scale bars represent 50 μm. GFP, green fluorescent protein; NLS, nuclear localization signal.

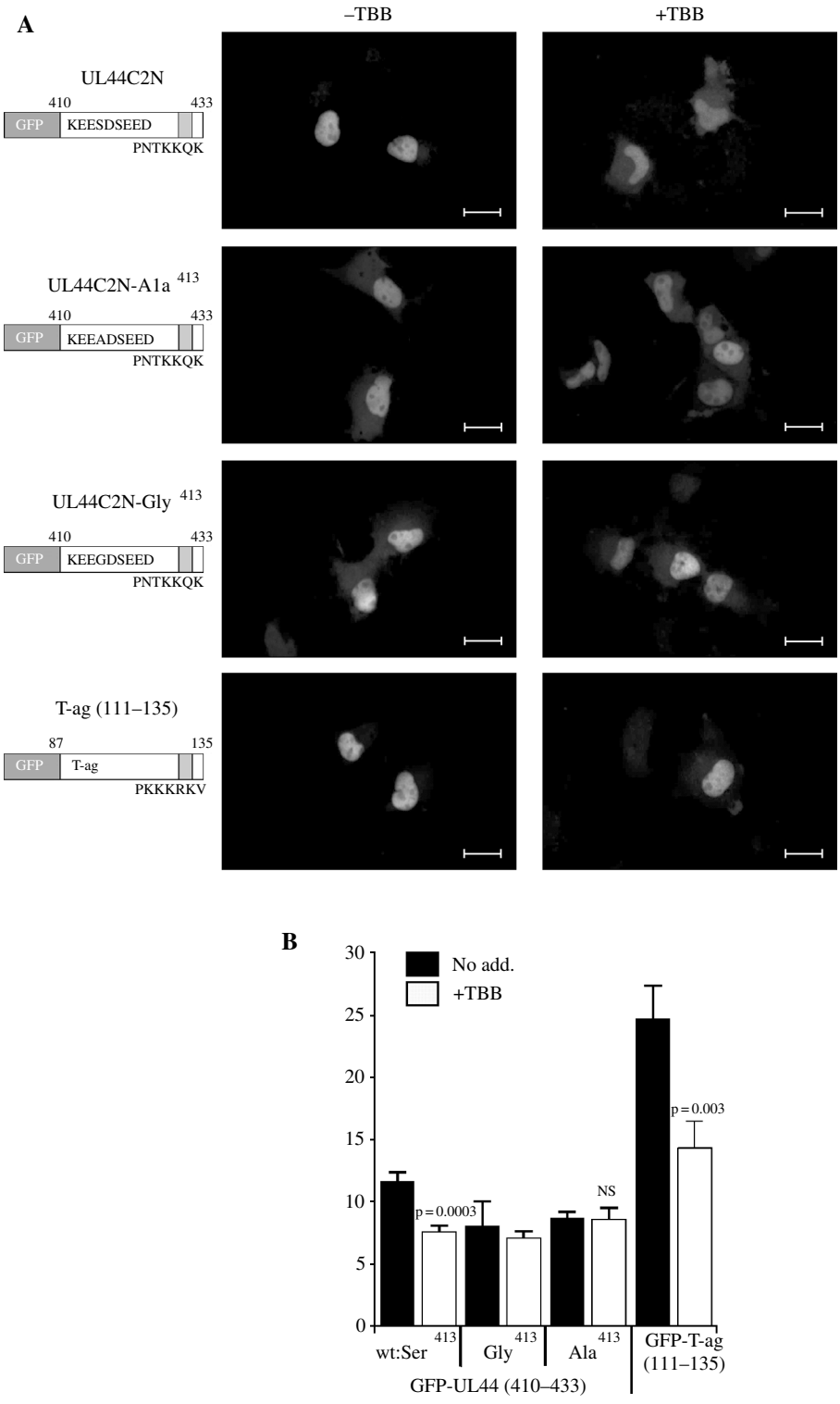

Figure 8: CK2 enhances ppUL44-NLS2 activity dependent on Ser^{413}. (A) COS-7 cells were transfected to express GFP fusion proteins and imaged live 16 h after transfection by using confocal laser scanning microscopy (CLSM) and a 40× water immersion objective. Just after transfection, 0.25% dimethyl sulphoxide (DMSO) (left panel) or 10 μM of TBB in 0.25% DMSO (right panel) was added. (B) Quantitative results for the nuclear to cytoplasmic ratio (Fn/c) for the GFP-UL44C2N fusion proteins. CLSM images such as those shown in Figure 8A were analysed as described in the legend to Figure 2. Data shown represent the mean ± SEM ($n > 40$) with p-values for the test of significance between the Fn/c-values for the indicated proteins in the presence and absence of TBB inhibitor shown. NS = not significant. Scale bars represent 50 μm. GFP, green fluorescent protein; NLS, nuclear localization signal; TBB, 4,5,6,7-tetrabromobenzotriazole.

To determine whether the basis of the enhancement of ppUL44-NLS2 action by the flanking sequences was through an improved binding by IMPα/β, as shown previously for T-ag and the CcN motif (23,24), gel mobility shift assays were performed to compare the IMP-binding properties of His_6GFP-UL44C2N and His_6GFP-UL44NLS2. The results indicated that His_6GFP-UL44C2N was able to bind both IMPα and α/β to a greater extent than His_6GFP-UL44NLS2 (Figure 9). The binding affinity of His_6GFP-UL44C2N for IMPα/β was calculated to be approximately

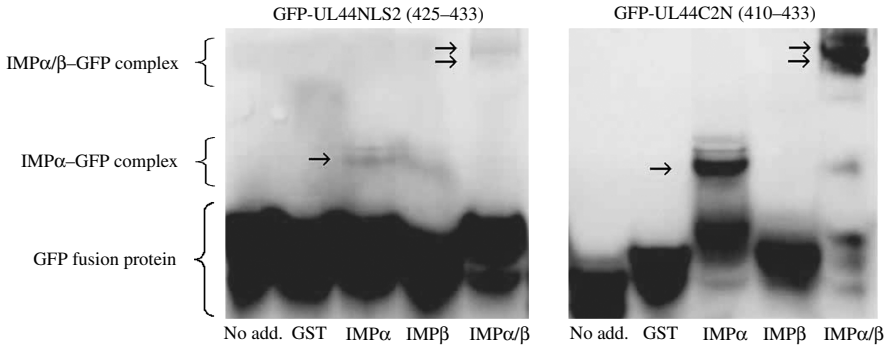

Figure 9: ppUL44-C2N binds importin (IMP) more efficiently than ppUL44-NLS2. The indicated GFP fusion proteins were incubated as described in *Materials and Methods* in the absence or presence of 10 μM of GST and GST-IMPs prior to native gel electrophoresis. Arrows indicate the positions of GFP fusion proteins and fusion protein–IMP complexes. GFP, green fluorescent protein; GST, glutathione *S*-transferase; NLS, nuclear localization signal.

170 nM (Figure 10), a value comparable to that recently reported for His_6GFP-T-ag-CcN and IMPα/β using native PAGE (30).

The estimated affinity of binding of IMPα/β to His_6GFP-UL44C2N based on the gel mobility shift technique was a higher K_d value than that estimated using the ELISA assay, consistent with the differing sensitivities of the two binding assays; the lower sensitivity of the native PAGE approach is attributable in part to dissociation of the protein–protein complex during electrophoretic movement through the gel (31,32).

That binding of IMPα/β to the C2N motif was dependent on NLS2 was supported by the finding that mutation of NLS2 severely impaired both ppUL44 nuclear localization and IMP-binding properties (Figures 1–5) and confirmed in competition experiments using the gel mobility shift assay. His_6GFP-UL44C2N incubation with IMPα/β was performed in the presence of either His_6UL44 or His_6UL44ΔNLS2, the results showing that His_6UL44 but not His_6UL44ΔNLS2 is able to compete for IMPα/β binding with His_6GFP-UL44C2N (Figure 11). The implication was that the enhancement by the flanking sequences of the C2N motif of IMPα/β binding and nuclear import mediated by the UL44NLS was not attributable to an additional NLS activity within the flanking sequences but rather was dependent on NLS2.

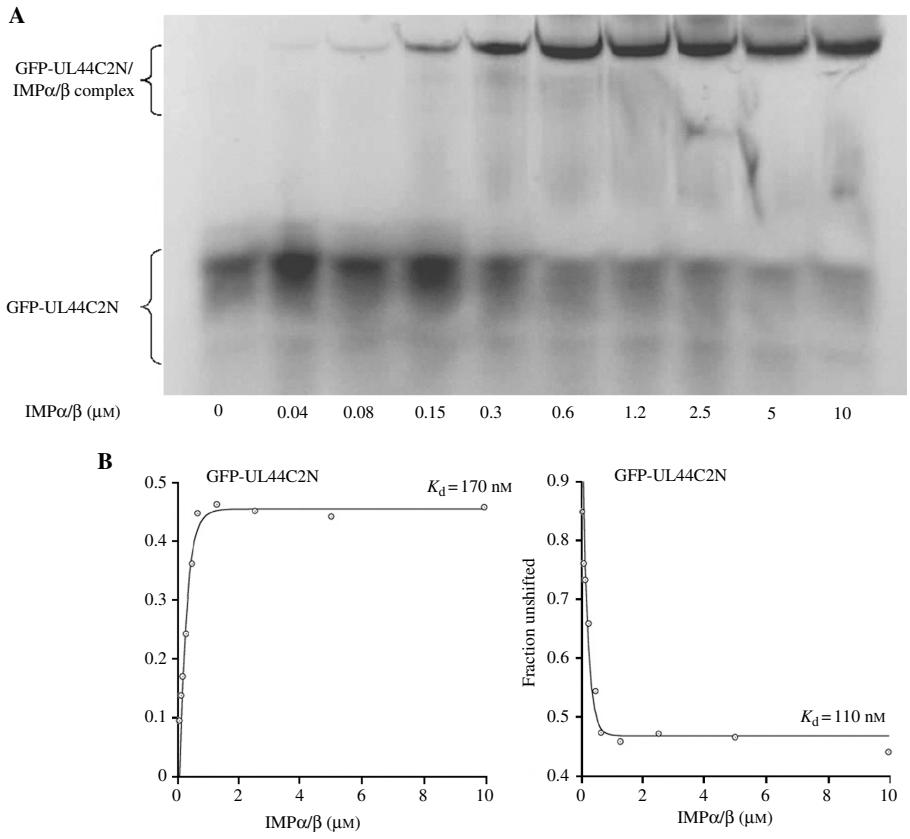

Figure 10: The IMPα/β heterodimer recognizes ppUL44-C2N with high affinity as shown by native PAGE/fluorimaging. (A) Fluorescent image of a native gel after electrophoresis for 8 h at 30 mA. The position of His_6GFP-UL44C2N (2 μM) is shown in the absence (lane 1) or presence (lanes 2–10) of preincubation with increasing amounts (0.04–10 μM) of precomplexed GST-mouse IMPα/β prior to native PAGE. (B) Results of quantitation of specific fluorescence from Figure 10A for the relative amount of His_6GFP-UL44C2N-shifted fluorescence due to IMP binding to the total fluorescence (left panel) and the relative amount of unshifted His_6GFP-UL44C2N is expressed as a ratio of the total fluorescence (right panel). The values for the apparent K_d representing the IMP concentration yielding half-maximal binding for shifted relative to total fluorescence ratio are indicated. GFP, green fluorescent protein; GST, glutathione *S*-transferase; IMP, importin. K_d, apparent dissociation constant; PAGE, polyacrylamide gel electrophoresis.

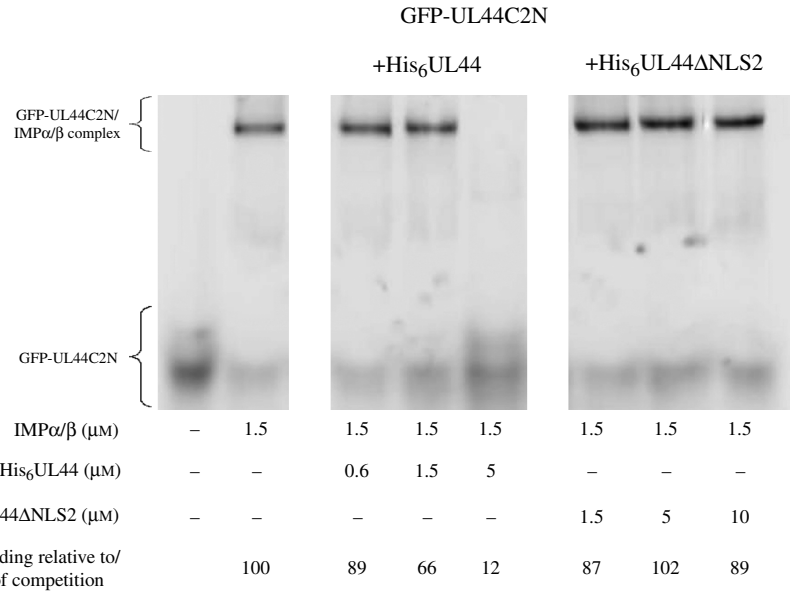

Figure 11: ppUL44-NLS2 is required for IMPα/β binding as shown by native polyacrylamide gel electrophoresis (PAGE). His_6GFP-UL44C2N (2 μM) was incubated alone (lane 1) or with 1.5 μM of pre-complexed GST-IMPα/β (lanes 2–8) in the presence of increasing amounts of His_6UL44 (lanes 3–5) or His_6UL44ΔNLS2 (lanes 6–8). Results are expressed as the percentage of maximal binding in the absence of added unlabelled UL44. Analysis was performed as described in the legend to Figure 10. GFP, green fluorescent protein; GST, glutathione *S*-transferase; IMP, importin; NLS, nuclear localization signal.

Discussion

We have characterized the nuclear import mechanism of ppUL44, defining the C2N motif, which appears to be highly conserved among several herpetic PAPs. This also represents the first quantitative analysis of the binding affinity of IMPα/β for an HCMV-encoded NLS. Results from a variety of *in vitro* assays and transfection experiments (Figures 1–5) show that ppUL44-NLS2, in contrast to ppUL44-NLS1, is sufficient and necessary for nuclear accumulation of ppUL44. Mutation of ppUL44-NLS2 results in cytoplasmic localization of ppUL44, in either full length or GFP-UL44 fusion protein contexts, with ppUL44-NLS2 alone sufficient to target GFP to the nucleus. Comparable experiments for ppUL44-NLS1 indicate that it is neither sufficient nor necessary for ppUL44 nuclear localization, although the mutation of ppUL44-NLS1 altered the localization pattern of ppUL44 within the nucleus, resulting in a loss of 'speckled' localization (see Figure 2A). We hypothesize that the speckled nuclear pattern observed with wild-type UL44 results from ppUL44 interacting with nuclear components; interaction with nuclear components has been hypothesized for HHV-7 U27 (15) and is consistent with the recent proposition that residues 163–174, spanning ppUL44-NLS1, are involved in DNA binding (33). Irrespective of whether the sequences mutated in ppUL44-NLS1 affect ppUL44 interaction with DNA or nuclear proteins, our results clearly support the conclusion that ppUL44-NLS2 but not ppUL44-NLS1 is required for nuclear localization of ppUL44.

ppUL44 is known to bind strongly to DNA once within the nucleus via residues 1–290 (4,5). It thus seems likely that nuclear retention contributes markedly to the ability of ppUL44 to accumulate in the nucleus. This increased nuclear retention is presumably the basis for the weaker nuclear accumulation we reported for the GFP-UL44NLS2 fusion protein, which lacks the DNA-binding domain, when compared to GFP-UL44.

Our binding results, performed using several different techniques, imply that ppUL44 is translocated to the nucleus through a conventional IMPα/β-mediated pathway conferred by NLS2, as supported by the ability of ppUL44-NLS2 to confer IMP-binding ability to GFP when fused to its C-terminus in gel mobility shift experiments. In ELISA assays, bacterially expressed wild-type UL44 and its NLS1-mutated derivative bound IMPα/β with higher affinity than IMPα, consistent with autoinhibition of NLS binding in IMPα in the absence of IMPβ (19). The finding that the NLS2-mutated derivative did not bind IMPs with high affinity is consistent with the idea that the cytoplasmic localization of NLS2-mutated ppUL44 in transfection experiments is a consequence of the lack of interaction with IMPα/β. In ELISA-based assays, the affinity of binding of ppUL44 to the IMPα/β heterodimer was calculated to be approximately 2 nM, a value comparable to that reported for T-ag and IMPα/β previously (23,24).

That the nuclear import of NLS-carrying proteins can be modulated by phosphorylation near to and within NLSs has been documented for a number of proteins. Phosphorylation-mediated regulation may enhance nuclear import, as in the case of T-ag and the synergistically acting CK2 and dsDNA-PK (23,24), or inhibit it, as in the case of T-ag and its cdk site (22), or the v-Jun protein, which shows cell cycle-dependent phosphorylation of a serine in position 1 of the NLS (34). The ppUL44-C2N motif (amino acids 410–433) possesses potential phosphorylation sites for CK2 at Ser^{413} and, eventually, in case Ser^{418} becomes phosphorylated, also at Ser^{415}, located at position −14 and −12 with respect to the NLS

core (see Figure 6), as well as a potential phosphorylation site at Thr^{427}, located at position 1 of the NLS core. The ability of these sequences to alter the properties of ppUL44-NLS2 was demonstrated in gel mobility shift assays, where ppUL44-C2N was found to confer higher-affinity interaction with IMPα/β than ppUL44-NLS2 alone. This higher-affinity binding is presumably the basis of the increased nuclear accumulation conferred by the ppUL44-C2N motif on GFP than the ppUL44-NLS2 alone. This conclusion is strengthened by the recent crystallographic demonstration that sequences N-terminal to the T-ag NLS participate directly in interaction with specific residues of IMPα (35).

The evidence that Ser^{413} is the likely target of CK2-mediated phosphorylation, which appears to enhance C2N activity in terms of nuclear import, strengthens the similarity between the ppUL44-C2N and T-ag CcN motifs. Substitution of Ser^{413} or treatment with TBB diminished, but did not abolish, the enhancing effect of flanking sequences on NLS2 activity, suggesting that C2N activity could be modulated by phosphorylation-effected changes in conformation affecting its ability to interact with IMPα. The implication is that action of CK2 on the C2N motif may play an important role in determining the ppUL44 nuclear import rate during viral infection. Future work in this laboratory is directed at investigating the effect of TBB-mediated CK2 inhibition on viral replication in infected cells.

Materials and Methods

Plasmid construction by conventional approaches

HCMV ORF UL44 sequence and the UL44ΔNLS2 mutant in which KKQK^{431} was replaced with VAQL were amplified by polymerase chain reaction (PCR), using appropriate primers and the HCMV Towne strain genome as a template, and subcloned into plasmid pCAP vector (Roche Diagnostics, Basel, Switzerland), to generate constructs pCAPUL44 and pCAPUL44ΔNLS2. Site-directed mutagenesis of pCAPUL44 was performed using the Quickchange™ mutagenesis kit (Stratagene, La Jolla, CA, USA) to generate plasmid pCAPUL44ΔNLS1 in which UL44 residues RVKR^{168} were substituted by GVNG. Fragments generated by digestion of the latter plasmids were cloned into plasmid vectors pCDNA3.1 and pRSETA (Invitrogen, Carlsbad, CA, USA), to generate mammalian cell and bacterial expression constructs, respectively.

To generate mammalian cell expression construct pHM830 T-ag, encoding a fusion protein with the T-ag NLS (PKKKRKV^{132}) between the coding sequence of GFP and β-Gal, an appropriate oligonucleotide pair was annealed and cloned into expression vector pHM830 (36).

GFP fusion protein expression plasmid construction using the Gateway™ technology

All prokaryotic and mammalian constructs expressing GFP-UL44 fusion proteins were generated using the Gateway™ system (Invitrogen). Primers including the attB1 and attB2 recombination sites were used to amplify the UL44 sequences of interest. PCR fragments were introduced into plasmid vector pDONOR207 (Invitrogen) via the BP recombination reaction, according to the manufacturer's recommendations, to generate the entry clones pDNR-UL44 (residues 2–433), pDNR-UL44ΔNLS1 (residues 2–433, GVNG^{168}), pDNR-UL44ΔNLS2 (residues 2–433, VAQL^{431}), pDNR-UL44NLS1 (residues 156–179), pDNR-UL44NLS1Δ (residues 156–179, GVNG^{168}), pDNR-UL44NLS2 (residues 425–433), pDNR-UL44NLS2Δ (residues 425–433, VAQL^{431}), pDNR-UL44C2N (residues 410–433), pDNR-UL44C2N (residues 410–433, Ala^{413}) and pDNR-UL44C2N (residues 410–433, Gly^{413}). The entry clone pDNR-T-ag-CcN, encoding T-ag residues 111–135, has been described previously (37). Entry clones were then used to perform LR recombination reactions with the Gateway system compatible expression plasmids ('DEST') pGFPrfB (37) and pDEST53 (Invitrogen) according to the manufacturer's recommendations. The integrity of all constructs was confirmed by DNA sequencing (MWG-BIOTECH, Ebersberg, Germany).

Cell culture and transfection

COS-7, U373-MG and HeLa cells were maintained in DMEM supplemented with 5% (v/v) foetal bovine serum, 50 U/mL of penicillin, 50 U/mL of streptomycin and 2 mM of L-glutamine. Cells were trypsinized and 4×10^4 cells were seeded onto coverslips in a 12-well multiwell plate 1 day before transfection, which was performed using Lipofectamine 2000 (Invitrogen), according to the manufacturer's recommendation.

According to the method described previously (38), TBB was synthesized; it was resuspended in DMSO and added to the cells after transfection at a final DMSO concentration of 0.25% (v/v). The integrity of expressed proteins was verified by Western blot as described previously (11).

Fluorescence microscopy and image analysis

Following fixation with 4% (w/v) paraformaldehyde, untagged UL44 proteins were visualized in transfected cells by using the mouse monoclonal antibody CH16 (Goodwin Institute, Plantation, FL, USA) and a fluorescein-labelled goat anti-mouse secondary antibody (Dako, Carpinteria, CA, USA). Samples were mounted on coverslips in PBS/glycerol (50% w/v) and imaged using a Nikon eclipse E600 fluorescence microscope equipped with a Nikon DXM 1200 digital camera and a Nikon Plan Fluor 40× objective (Nikon, Tokyo, Japan). Subcellular localization of GFP-UL44 fusion proteins in living cells was visualized 16 h after transfection by CLSM (BioRAD MRC500, BioRad Laboratories, Hercules, CA), using a Nikon 40× water immersion lens. The Fn/c was determined as described previously (23,24) using the IMAGE J 1.62 public domain software (NIH), from single cell measurements for each of the nuclear (Fn) and cytoplasmic (Fc) fluorescence, subsequent to the subtraction of fluorescence due to autofluorescence/background.

Expression and purification of His_6- and glutathione S-transferase-tagged fusion proteins

The His_6UL44, His_6UL44ΔNLS1 and His_6UL44ΔNLS2 proteins were expressed in *Escherichia coli* strain BL21 (DE3), while His_6GFP-UL44NLS1, His_6GFP-UL44NLS2 and His_6GFP-UL44C2N were expressed in *E. coli* strain M15 carrying plasmid pREP4, essentially as described previously (37,39). Protein expression was induced for 6 h with isopropyl β-D-thiogalactoside (1 mM) at 28 °C, and proteins were purified by nickel-affinity chromatography, as described previously (39). Expression and purification of glutathione *S*-transferase (GST)-tagged mouse IMPs α1 and β1 was performed as described previously (23).

Gel mobility shift assay

To test the ability of IMPs to bind UL44, native PAGE/fluorimaging was used as described previously (37,39). GFP fusion proteins (2 μM) were incubated for 15 min at room temperature with different concentrations of mouse IMPα-GST, IMPβ-GST, precomplexed IMPα/IMPβ-GST [performed as described previously (23)] or GST as a control in PBS. Competition experiments between His_6UL44 or His_6UL44ΔNLS2 and His_6GFP-UL44C2N for IMPα/β binding were performed as follows: different concentrations of His_6UL44 and His_6UL44ΔNLS2 were preincubated for 15 min at room temperature with 1.5 μM of IMPα/β heterodimer, and then His_6GFP-UL44C2N was added to a final concentration of 2 μM to the reaction and incubated for a further 15 min at room temperature. Sucrose was added to reactions to a final concentration of 15% (w/v), and the mixture was electrophoresed at 30 V for 8 h on a native PAGE 4–20% gradient gel (Gradipore, Frenchs Forest, NSW, Australia) run in TBE buffer. The gels were visualized using a Wallac Arthur 1422 Multi-wavelength Fluorimager (Perkin Elmer, Boston, MA, USA), using side illumination, and exposure times of 0.25–2 seconds. Digital images so obtained were

analysed using IMAGE J 1.62 software (39), where the fluorescence of the shifted band(s) was expressed as a fraction of the total fluorescence within the lane of the gel, subsequent to the subtraction of background fluorescence. Data were plotted and fitted using the KALEIDAGRAPH 2.1 software (Synergy Software, Reading, PA, USA).

ELISA binding assay

An established ELISA-based binding assay (23,24,40) was used to examine the binding affinity between IMPs and His_6UL44, His_6UL44ΔNLS1 and His_6UL44ΔNLS2. Briefly, 96-well microtitre plates (Nunc, Denmark) were coated with 5 pmol of protein per well and incubated with increasing concentrations of GST-IMP subunits. Detection of bound IMP-GST was performed using a goat anti-GST primary antibody (Pharmacia Biotech Inc., Piscataway, NJ, USA), an alkaline phosphatase-coupled rabbit anti-goat secondary antibody (SIGMA, St Louis, MO, USA) and *p*-nitrophenyl phosphate (SIGMA) as substrate. Absorbance measurements at 405 nm were performed over 90 min using a plate reader (Molecular Devices, Sunnyvale, CA, USA), with values corrected by subtracting absorbance both at 0 min and in wells incubated without IMPs. Data were fitted to the function $B(x) = B_{max}(1 - e^{-kB})$, where x is the concentration of IMP, k is the rate constant and B is the level of bound IMP.

Analysis of sequence motifs within ppUL44

Putative NLS sequences and phosphorylation sites within the ppUL44 coding sequence were identified using the PSORTII (28) and the NETPHOS (41) softwares, respectively.

Acknowledgments

This work was partly supported by the University of Bologna and the Italian Ministry of Education (60% and 40%, respectively), by the AIDS Project of the Italian Ministry of Public Health and by the Australian National Health and Medical Research Council (fellowship no.143790/333013 and project grant no. 143710 to DAJ). C.L. Barton and M.M. Dias are thanked for skilled technical assistance, T. Stamminger (Erlangen) for providing the pHM830 construct, S. Varani and G. Frascaroli for critical reviewing of the manuscript and M. Marschall (Erlangen) for helpful discussions.

References

1. Alford CA, Stagno S, Pass RF, Britt WJ. Congenital and perinatal cytomegalovirus infections. Rev Infect Dis 1990;12(Suppl. 7):S745–S753.
2. Anders DG, McCue LA. The human cytomegalovirus genes and proteins required for DNA synthesis. Intervirology 1996;39:378–388.
3. Pari GS, Anders DG. Eleven loci encoding trans-acting factors are required for transient complementation of human cytomegalovirus oriLyt-dependent DNA replication. J Virol 1993;67:6979–6988.
4. Mocarski ES, Pereira L, Michael N. Precise localization of genes on large animal virus genomes: use of lambda gt11 and monoclonal antibodies to map the gene for a cytomegalovirus protein family. Proc Natl Acad Sci USA 1985;82:1266–1270.
5. Weiland KL, Oien NL, Homa F, Wathen MW. Functional analysis of human cytomegalovirus polymerase accessory protein. Virus Res 1994;34:191–206.
6. Marschall M, Freitag M, Suchy P, Romaker D, Kupfer R, Hanke M, Stamminger T. The protein kinase pUL97 of human cytomegalovirus interacts with and phosphorylates the DNA polymerase processivity factor pUL44. Virology 2003;311:60–71.
7. Krosky PM, Baek MC, Jahng WJ, Barrera I, Harvey RJ, Biron KK, Coen DM, Sethna PB. The human cytomegalovirus UL44 protein is a substrate for the UL97 protein kinase. J Virol 2003;77:7720–7727.
8. Gibson W, Murphy TL, Roby C. Cytomegalovirus-infected cells contain a DNA-binding protein. Virology 1981;111:251–262.
9. Ertl PF, Powell KL. Physical and functional interaction of human cytomegalovirus DNA polymerase and its accessory protein (ICP36) expressed in insect cells. J Virol 1992;66:4126–4133.
10. Pari GS, Kacica MA, Anders DG. Open reading frames UL44, IRS1/TRS1, and UL36-38 are required for transient complementation of human cytomegalovirus oriLyt-dependent DNA synthesis. J Virol 1993;67:2575–2582.
11. Ripalti A, Boccuni MC, Campanini F, Landini MP. Cytomegalovirus-mediated induction of antisense mRNA expression to UL44 inhibits virus replication in an astrocytoma cell line: identification of an essential gene. J Virol 1995;69:2047–2057.
12. Mocarski ES. Cytomegalovirus. In: Roizman B, Whitley RJ, Lopez C, editors. The Human Herpesviruses. New York: Raven Press; 1993, pp. 173–226.
13. Loregian A, Appleton BA, Hogle JM, Coen DM. Specific residues in the connector loop of the human cytomegalovirus DNA polymerase accessory protein UL44 are crucial for interaction with the UL54 catalytic subunit. J Virol 2004;78:9084–9092.
14. Boccuni MC, Campanini F, Battista MC, Bergamini G, Dal Monte P, Ripalti A, Landini MP. Human cytomegalovirus product UL44 down-regulates the transactivation of HIV-1 long terminal repeat. AIDS 1998;12:365–372.
15. Takeda K, Haque M, Nagoshi E, Takemoto M, Shimamoto T, Yoneda Y, Yamanishi K. Characterization of human herpesvirus 7 U27 gene product and identification of its nuclear localization signal. Virology 2000;272:394–401.
16. Loh LC, Keeler VD, Shanley JD. Sequence requirements for the nuclear localization of the murine cytomegalovirus M44 gene product pp50. Virology 1999;259:43–59.
17. Jans DA, Xiao CY, Lam MH. Nuclear targeting signal recognition: a key control point in nuclear transport? Bioessays 2000;22:532–544.
18. Kalderon D, Richardson WD, Markham AF, Smith AE. Sequence requirements for nuclear location of simian virus 40 large-T antigen. Nature 1984;311:33–38.
19. Kobe B. Autoinhibition by an internal nuclear localization signal revealed by the crystal structure of mammalian importin alpha. Nat Struct Biol 1999;6:388–397.
20. Jans DA, Hubner S. Regulation of protein transport to the nucleus: central role of phosphorylation. Physiol Rev 1996;76:651–685.
21. Jans DA, Jans P. Negative charge at the casein kinase II site flanking the nuclear localization signal of the SV40 large T-antigen is mechanistically important for enhanced nuclear import. Oncogene 1994;9:2961–2968.
22. Jans DA, Ackermann MJ, Bischoff JR, Beach DH, Peters R. p34cdc2-mediated phosphorylation at T124 inhibits nuclear import of SV-40 T antigen proteins. J Cell Biol 1991;115:1203–1212.
23. Hubner S, Xiao CY, Jans DA. The protein kinase CK2 site (Ser111/112) enhances recognition of the simian virus 40 large T-antigen nuclear localization sequence by importin. J Biol Chem 1997;272:17191–17195.
24. Xiao CY, Hubner S, Jans DA. SV40 large tumor antigen nuclear import is regulated by the double-stranded DNA-dependent protein kinase site (serine 120) flanking the nuclear localization sequence. J Biol Chem 1997;272:22191–22198.
25. Zhang Q, Holley-Guthrie E, Dorsky D, Kenney S. Identification of transactivator and nuclear localization domains in the Epstein-Barr virus DNA polymerase accessory protein, BMRF1. J Gen Virol 1999;80:69–74.
26. Gerdes HH, Kaether C. Green fluorescent protein: applications in cell biology. FEBS Lett 1996;389:44–47.
27. Pinna LA. Protein kinase CK2: a challenge to canons. J Cell Sci 2002;115:3873–3878.
28. Horton P, Nakai K. Better prediction of protein cellular localization sites with the k nearest neighbors classifier. Proc Int Conf Intell Syst Mol Biol 1997;5:147–152.
29. Sarno S, Reddy H, Meggio F, Ruzzene M, Davies SP, Donella-Deana A, Shugar D, Pinna LA. Selectivity of 4,5,6,7-tetrabromobenzotriazole, an

ATP site-directed inhibitor of protein kinase CK2 ('casein kinase-2'). FEBS Lett 2001;496:44–48.
30. Wagstaff KM, Dias MM, Alvisi G, Jans DA. Quantitative analysis of protein-protein interactions by native page/fluorimaging. J Fluoresc 2005;15:469–473.
31. Park SH, Raines RT. Green fluorescent protein as a signal for protein-protein interactions. Protein Sci 1997;6:2344–2349.
32. Forwood JK, Lam MH, Jans DA. Nuclear import of Creb and AP-1 transcription factors requires importin-beta 1 and Ran but is independent of importin-alpha. Biochemistry 2001;40:5208–5217.
33. Appleton BA, Loregian A, Filman DJ, Coen DM, Hogle JM. The cytomegalovirus DNA polymerase subunit UL44 forms a C clamp-shaped dimer. Mol Cell 2004;15:233–244.
34. Tagawa T, Kuroki T, Vogt PK, Chida K. The cell cycle-dependent nuclear import of v-Jun is regulated by phosphorylation of a serine adjacent to the nuclear localization signal. J Cell Biol 1995;130:255–263.
35. Fontes MR, Teh T, Toth G, John A, Pavo I, Jans DA, Kobe B. Role of flanking sequences and phosphorylation in the recognition of the simian-virus-40 large T-antigen nuclear localization sequences by importin-alpha. Biochem J 2003;375:339–349.
36. Sorg G, Stamminger T. Mapping of nuclear localization signals by simultaneous fusion to green fluorescent protein and to beta-galactosidase. Biotechniques 1999;26:858–862.
37. Baliga BC, Colussi PA, Read SH, Dias MM, Jans DA, Kumar S. Role of prodomain in importin-mediated nuclear localization and activation of caspase-2. J Biol Chem 2003;278:4899–4905.
38. Szyszka R, Grankowski N, Felczak K, Shugar D. Halogenated benzimidazoles and benzotriazoles as selective inhibitors of protein kinases CK I and CK II from Saccharomyces cerevisiae and other sources. Biochem Biophys Res Commun 1995;208:418–424.
39. Forwood JK, Harley V, Jans DA. The C-terminal nuclear localization signal of the sex-determining region Y (SRY) high mobility group domain mediates nuclear import through importin beta 1. J Biol Chem 2001;276:46575–46582.
40. Hu W, Jans DA. Efficiency of importin alpha/beta-mediated nuclear localization sequence recognition and nuclear import. Differential role of NTF2. J Biol Chem 1999;274:15820–15827.
41. Blom N, Gammeltoft S, Brunak S. Sequence and structure-based prediction of eukaryotic protein phosphorylation sites. J Mol Biol 1999;294:1351–1362.